48/2010

# Raport Badawczy
# Research Report

**RB/12/2010**

# A model for mechanical compaction of the Upper Jurassic bedded limestones

**J. Jarnicka, A. Kochman**

**Instytut Badań Systemowych**
**Polska Akademia Nauk**

**Systems Research Institute**
**Polish Academy of Sciences**

# POLSKA AKADEMIA NAUK

## Instytut Badań Systemowych

ul. Newelska 6

01-447 Warszawa

tel.: (+48) (22) 3810100

fax: (+48) (22) 3810105


Kierownik Pracowni zgłaszający pracę:
Prof. dr hab. inż. Zbigniew Nahorski

Warszawa 2010

Mathematical Geosciences manuscript No.
(will be inserted by the editor)

# A model for mechanical compaction of the Upper Jurassic bedded limestones

Jolanta Jarnicka · Alicja Kochman

the date of receipt and acceptance should be inserted later

**Abstract** Determination of the compaction of the carbonate sediments presents the basic difficulty at evaluation of their post-depositional thickness. Oedometric experiments were carried out for the samples prepared from fine-detrital, intra-biohermal facies of the Upper Jurassic from the Krakow-Czestochowa Upland. The relationships between the burden of samples, of which grain composition simulated sediments from a natural outcrop, and changes in the sample heights were subjected to the mathematical modelling. A parametric model was proposed. The power function turned out to be the one providing the best fit. To fit the model to the data given, the regression analysis was used. The model was linearized and the parameters were estimated, using the least squares method. The model proposed reflects the impact of the mechanical compaction on the present thickness of the carbonate sediments, assuming lack of early-diagenetical cementation of the sediments discussed.

**Keywords** mechanical compaction · carbonate rocks · model fitting · parametric estimation

## 1 Introduction

Compaction is one of the main processes leading to a reduction of carbonate deposits in thickness ([3],[10], and [29]). There are two types of compaction: mechanical (physical) and chemical; in this paper the first one is considered.

J. Jarnicka
Systems Research Institute, Polish Academy of Sciences, Warsaw, 01-447, Newelska 6,
E-mail: Jolanta.Jarnicka@ibspan.waw.pl

A. Kochman
Faculty of Geology, Geophysics and Environment Protection, AGH University of Science and Technology, Cracow, 30-059, Mickiewicza 30,
E-mail: kochman@geol.agh.edu.pl

The mechanical compaction, closely following the deposition processes, continuously affects the sediments deposited and buried until their total lithification, however, with decreasing intensity strength ([13], [12], and [22]). The sediment lithification is a conventional boundary between the early diagenesis and burial diagenesis stages.

Mechanical compaction, above all, leads to an increase of the grain density in the sediment, (see [5]), which, in turn, results in its dehydration as well as and a reduction in porosity and permeability ([2], [3], [23], [1], [12], and [22]). Apart from densification of the skeletal grains, the mechanical compaction may also bring about breaking and small displacement of the sediment grains ([2], [6], and [22]).

The chemical compaction takes place in a lithified sediments, at the pressures exerted by a sediment pile of a thickness reaching at least 200 – 250 m ([27],[11], and [7]). This type of compaction also causes a reduction in thickness of the carbonate rocks, connected with pressure dissolution processes, occurring in the lithified rock.

Depending on the deposition conditions and the burial depth, the sediments are subjected to differential compaction - an essential element in the reconstruction of the facies architecture of sedimentary basins, filled with sediments of varying susceptibility to the mechanical compaction, as well as some unsusceptible to it ([13], [26], and [25]).

While determination of the impact of the mechanical compaction on the sediment is documented with easily readable textures, quantitative characteristics of this process is quite complicated, because of complexity of the geological processes. Quantitative determination of the thickness reduction of the carbonate deposits due to the mechanical compaction has been attempted on the basis of the results of laboratory tests or computational algorithms, taking into account several factors, such as presumable chemical composition of the sediment, chemical composition of the rock formed by the sediment compaction, primary and presents porosity, as well as probable thickness of the overlying sediments ([28], [23], [24], [8], [12], [30], [14], and [15]).

This paper presents a mathematical approach to the results of the model tests on the mechanical compaction of the fine-detrital carbonate sediments, deposited in the sedimentary basin covering the Krakow-Czestochowa Upland in the Late Jurassic period (see [16]).

## 2 Geological setting

In the Cracow-Częstochowa Upland the Upper Jurassic carbonate rocks are represented by three main types of facies: (i) massive limestones, (ii) bedded limestones, and (iii) gravity flow deposits ([9], and [19]). Their diverse lithology points out diverse susceptibility to the mechanical compaction. Massive limestones, representing the Upper Jurassic carbonate buildups, were not subjected to the mechanical compaction, because of their rigid framework, mostly built by microbolites, as well as early diagenetic cementation processes. On the other hand, the mechanical compaction affected the bedded limestones and gravity flow deposits, in which the early cementation processes occurred more slowly, due to lack of the rigid framework and high content of clays. The increased clay content prevented early cementation, leading to slowing of the sediment lithification ([4]). Differential compaction, is considered as one of the reasons for the present local inclination of the limestone layers surrounding carbonate buildups, and also for significant differences in thickness between the massive facies and bedded limestones, deposited in the same time interval (see [20]).

## 3 Methodology

Mechanical compaction of the Upper Jurassic bedded limestones was investigated on samples taken from the outcrop in Zary near Krzeszowice. This outcrop exhibits bedded limestones, formed between the carbonate buildups, unsusceptible to the mechanical compaction ([17], and [21]).

The research method used was the oedometric analysis of compressibility, aimed at determination of the relationships between the load imposed on a sample during the oedometric tests and variations in its height. The decrease in the sample height can be interpreted, with some restrictions, as a compactive reduction in the sediment thickness. The samples subjected to the laboratory tests have been prepared in such a way that their grain composition corresponded to the Upper Jurassic bedded limestones, observed in the outcrop in Zary. For the purpose of the experiment, a special model of the oedometric tests was developed, in which each of the following samples was subjected to a load simulating various burial depths (see [16] for details).

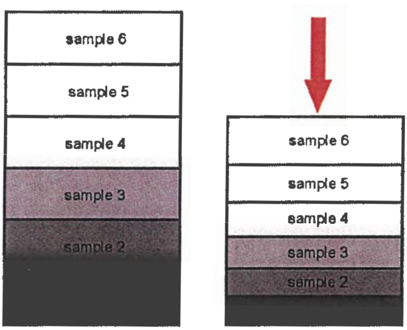


**Fig. 1.** Model profile (with positions of the subsequently analysed samples), for which the oedometric tests were carried out (assumed situation before and after compaction).

It was assumed that 6 samples would create a model profile (Fig. 1), in which the sample 1 corresponded to the lowermost layer, affected by the burden of the samples 2 – 6. Sample 2 was deformed under the load of the samples 3 – 6, sample 3 - under the load of the samples 4 – 6, etc. The burden applied to the sample 6, representing the top layer, was supposed to simulate the pressure exerted by the overburden of the Upper Jurassic sediments.

In order to simulate the continuity of the mechanical compaction, the load was gradually being changed. The results obtained from the oedometric studies are presented in Tables 1 – 6.

| load [kPa] | height [mm] |
|---|---|
| 0 | 33.64 |
| 2.78 | 27.74 |
| 41.57 | 25.64 |
| 41.57 | 25.64 |
| 83.87 | 23.895 |
| 83.87 | 23.89 |
| 168.45 | 23.35 |
| 168.45 | 23.34 |
| 336.35 | 22.835 |
| 336.35 | 22.815 |

**Table 1**. Height of the sample 1, depending on the load applied.

| load [kPa] | height [mm] |
|---|---|
| 0 | 32.08 |
| 2.55 | 26.92 |
| 33.73 | 24.16 |
| 33.73 | 24.14 |
| 76.03 | 23.72 |
| 76.03 | 23.705 |
| 155.55 | 23.19 |
| 155.55 | 23.165 |
| 323.45 | 22.665 |
| 323.45 | 22.63 |

**Table 2**. Height of the sample 2, depending on the load applied.

| load [kPa] | height [mm] |
|---|---|
| 0 | 45.15 |
| 2.78 | 38.64 |
| 21.15 | 32.965 |
| 21.15 | 32.955 |
| 63.45 | 31.97 |
| 63.45 | 31.965 |
| 147.15 | 31.255 |
| 147.15 | 31.25 |
| 315.05 | 30.69 |
| 315.05 | 30.64 |

**Table 3**. Height of the sample 3, depending on the load applied.

| load [kPa] | height [mm] |
|---|---|
| 0 | 35.22 |
| 2.55 | 29.64 |
| 42.30 | 24.21 |
| 42.30 | 24.20 |
| 126.00 | 23.45 |
| 126.00 | 23.425 |
| 293.90 | 22.61 |
| 293.90 | 22.56 |

**Table 4.** Height of the sample 4, depending on the load applied.

| load [kPa] | height [mm] |
|---|---|
| 0 | 41.42 |
| 2.78 | 34.90 |
| 83.70 | 29.75 |
| 83.70 | 29.71 |
| 251.90 | 29.16 |
| 251.90 | 29.15 |

**Table 5.** Height of the sample 5, depending on the load applied.

| load [kPa] | height [mm] |
|---|---|
| 0 | 41.37 |
| 2.55 | 34.69 |
| 167.90 | 29.94 |
| 167.90 | 29.93 |

**Table 6.** Height of the sample 6, depending on the load applied.

The data from tables 1 – 5 were used for a mathematical model, showing the relationship between the load and the sample height. Sample 6, due to too small size, has been omitted. Figure 2 presents the data from the samples 1 – 5 in the graphical form.

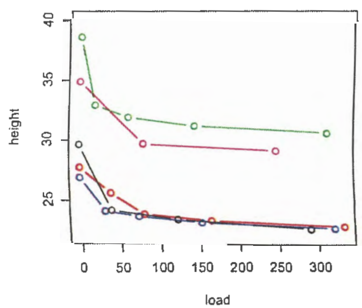


**Fig. 2.** Graphical illustration of the samples 1 – 5.

## 4 Model-fitting with regression

Regression analysis is used for explaining or modelling the relationship between a single variable $Y$, called the *dependent variable*, and one or more *independent variables* $X_1, X_2, \ldots, X_n$. Given a set of observations, it is based on finding the function $f$, which describes the relationship

$$Y = f(\mathbf{X}) + \varepsilon,$$

where $\mathbf{X} = (X_1, X_2, \ldots, X_n)$ and $\varepsilon$ is a random error. This can be done using a parametric estimation, based on the assumption of a model (i.e. assumption of the form of the estimated function) and then fit it to the data through the estimation of parameters, or using non-parametric regression methods (such as cross-validation methods, etc.) Due to the small sample size, we will focus on regression-based parametric estimation.

Most commonly used is a linear model, given by

$$\mathbf{y} = \mathbf{X}\beta + \varepsilon,$$

with parameters $\beta_i, i = 0, \ldots, k$, where

$$\mathbf{y} = (y_1, y_2, \ldots, y_n)^T, \quad \varepsilon = (\varepsilon_1, \varepsilon_2, \ldots, \varepsilon_n)^T, \quad \mathbf{X} = \begin{bmatrix} 1 & X_{11} & \ldots & X_{1n} \\ 1 & X_{21} & \ldots & X_{2n} \\ \ldots & \ldots & \ldots & \ldots \\ 1 & X_{k1} & \ldots & X_{kn} \end{bmatrix}.$$

Estimates of parameters $\beta = (\beta_0, \beta_1, \ldots, \beta_k)^T$, can be obtained from the least-squares method, as the ones minimizing $\varepsilon^T\varepsilon = (\mathbf{y} - \mathbf{X}\beta)^T(\mathbf{y} - \mathbf{X}\beta)$, i.e.

$$\widehat{\beta} = (\mathbf{X}^T\mathbf{X})^{-1}\mathbf{X}^T\mathbf{y},$$

if the errors $\varepsilon$ are normally distributed, uncorrelated and have equal variance. Then we obtain

$$\widehat{\mathbf{y}} = \mathbf{X}\widehat{\beta}, \qquad \widehat{\varepsilon} = \mathbf{y} - \widehat{\mathbf{y}}.$$

The data presented in Figure 2 indicate, however, that a nonlinear model should be applied. Let us therefore consider the simplest nonlinear models - one that can be linearized. Examples of such models, for the data from sample 1 are depicted in Figures 3(a) - (d).

The analysis carried out for some of the most popular models and comparison of their goodness of fit (the coefficients $R^2$ are respectively 60%, 94%, 53%, and 54%), show that the model provides the best fit for the power function.

$$y = aX^b \tag{1}$$

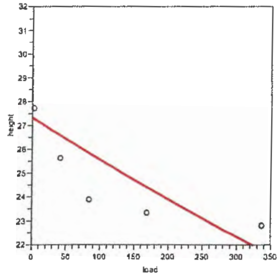


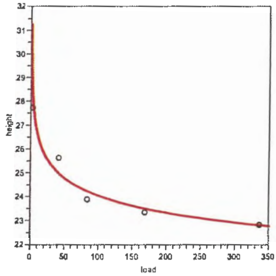


(a) $Y = e^{a+bX}$

(b) $Y = aX^b$

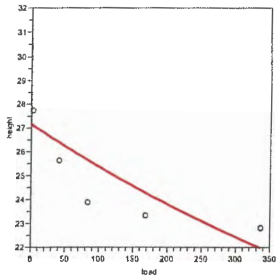


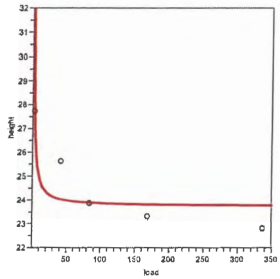


(c) $Y = \frac{1}{a+bX}$

(d) $Y = a + \frac{b}{X}$

**Fig. 3.** (a), (b), (c), and (d). Examples of nonlinear models fitted to the sample 1.

After log-transforming, model (1) becomes

$$\ln(y) = \ln(a) + b\ln(X),$$

where $a > 0$, so we obtain a linear model

$$y_1 = a_1 + bX_1, \tag{2}$$

with parameters $a_1$ and $b$. This means that we are looking for the regression line $y_1 = a_1 + bx_1$.

For the model chosen, it is necessary to satisfy the condition $X_i > 0$ and $y_i > 0$, therefore, in samples 1 – 5 (Tables 1 – 5) we have to skip the first pair of observations.

The analysis of the data from sample 1, with the use of `R, version 2.7.2`, gives the following result.

```
Coefficients:
             Estimate Std. Error t value Pr(>|t|)
(Intercept)  3.380205   0.018600  181.73 4.03e-14 ***
log(obc1)   -0.043519   0.004066  -10.70 1.36e-05 ***
---
Signif. codes:  0 '***' 0.001 '**' 0.01 '*' 0.05 '.' 0.1 ' ' 1
Residual standard error: 0.01695 on 7 degrees of freedom
Multiple R-squared: 0.9424,     Adjusted R-squared: 0.9342
F-statistic: 114.6 on 1 and 7 DF,  p-value: 1.365e-05
```

The estimates for parameters in (2) are equal $\widehat{a}_1 = 3.380205$, and $\widehat{b} = -0.043519$, with standard errors 0.018600 and 0.004066. Hence, we obtain the regression line

$$\widehat{y}_1 = 3.38 - 0.044x_1.$$

Now, we check the fit of the model. The $R^2$ is equal 94%, which indicates a good fit to the data. Tests of significance of coefficients $a_1$ and $b$, give very small p-values, so in both cases, we reject a hypothesis that they are statistically insignificant. Similarly, F-test, shows a linear dependence of the variables tested, by rejecting the hypothesis (since $p - value = 1.365 \cdot 10^{-5}$), that their relationship cannot be described by a linear model.

To confirm the results obtained, it is still necessary to test the normality of residuals in the model fitted.

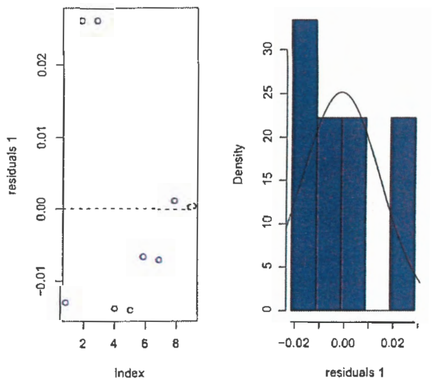


**Fig. 4.** Scatter plot of residuals. Histogram of residuals, the sample 1.

The Shapiro-Wilk normality test of the residuals (presented in Fig. 4), gives $p - value = 0.0598$ so, there is no reason to reject the hypothesis, that the distribution of residuals is normal.

Finally, we get the power function (1) of the form $\widehat{y} = 29.38X^{-0.044}$, where $\widehat{a} = \exp(\widehat{a}_1) = 29.38$. The result obtained is presented in Fig. 5.

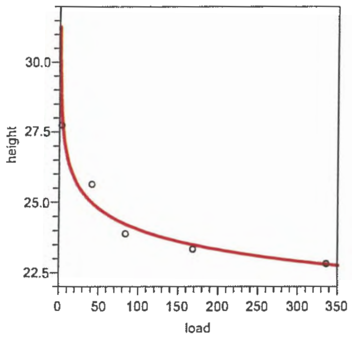


**Fig. 5.** Sample 1 with the fitted power function $\widehat{y} = 29.38X^{-0.044}$.

95%-confidence intervals for coefficients $a$ and $b$, respectively, are of the form (28.11274, 30.69768), and (−0.05313356, −0.03390444).

The analysis of samples 2 – 5, we perform similarly. The results obtained are shown in Figures 6 – 9.

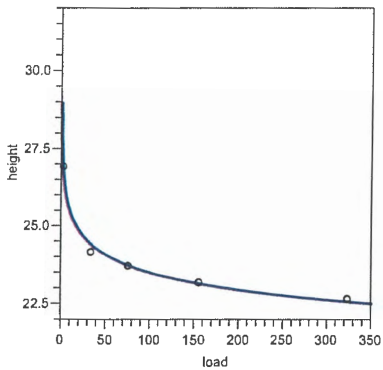


**Fig. 6.** Sample 2 with the fitted power function $\widehat{y} = 27.55825X^{-0.034654}$.

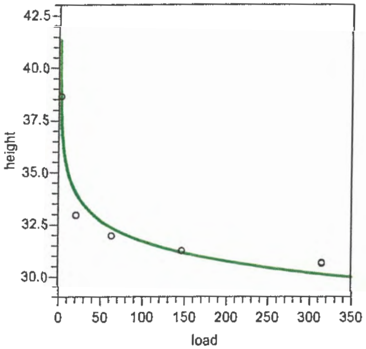


**Fig. 7**. Sample 3 with the fitted power function $\widehat{y} = 38.82716X^{-0.044083}$.

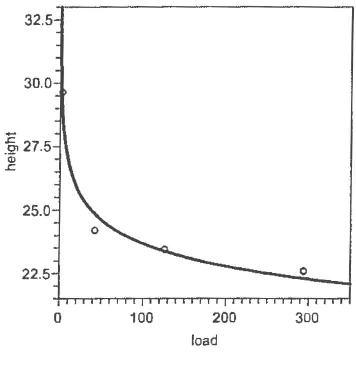


**Fig. 8**. Sample 4 with the fitted power function $\widehat{y} = 30.60685X^{-0.055764}$.

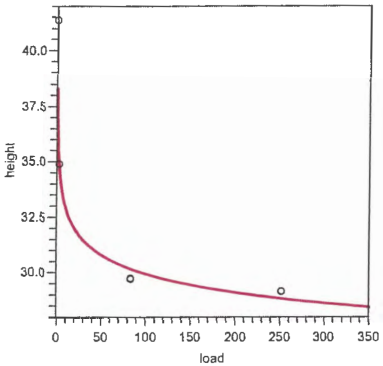


**Fig. 9**. Sample 5 with the fitted power function $\widehat{y} = 36.12904X^{-0.040766}$.

Figure 10, below, shows all the power functions obtained. For the convenience of reader, the colour of each function corresponds to that from Figures 7 − 9.

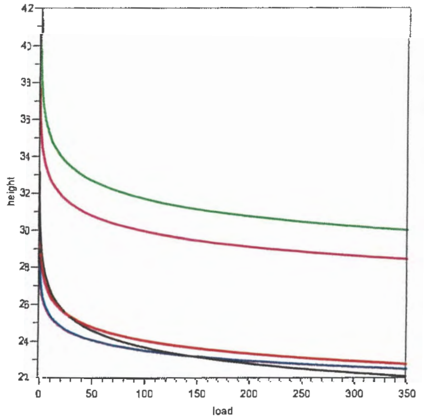


**Fig.10**. Power functions fitted to samples 1 − 5.

## 5 Conclusions

Based on a mathematical model, the mechanical compaction may be quantitatively evaluated, according to the equation

$$K = \left(1 - \frac{Y_{\max}}{Y_{\min}}\right) \cdot 100,$$

where

$K$ denotes mechanical compaction, expressed in [%],
$Y_{\max} = aX^b_{\max}$ (present thickness),
$Y_{\min} = aX^b_{\min}$ (initial thickness),

for $a \in (27.09; 41.16)$, $b \in (-0.068; -0.027)$.

Minimal and maximal load may be expressed through the overburden thickness of a layer, which, in turn, may be approximately evaluated, e.g. on the basis of the sedimentation or accumulation rate (see [18] and [6]). At the beginning, the sediment deposited would be subjected only to the minimal load $X_{\min} = 0.01$, where the condition $X_{\min} > 0$ fulfilled the requirement of the mathematical model, and $X_{\max}$ corresponded to the maximal load bringing about the mechanical compaction, until the sediment lithification.

The above formula does not take into account the chemical compaction.

## References


1. Audet D.M., 1995, *Modelling of porosity evolution and mechanical compaction of calcareous sediments*, Sedimentology, 42: 355-373.
2. Bathurst R.G.C., 1975, *Carbonate Sediments and their Diagenesis*, Elsevier Science Publ., Amsterdam, 1-658.
3. Bathurst R.G.C., 1987, *Diagenetically enhanced bedding in argillaceous platform limestone: stratified cementation and selective compaction*, Sedimentology, 34: 749-779.
4. Bausch W.M., 1996, *Noncarbonates as controlling factor in reef growth and as tool in reef stratigraphy (examples from the Upper Jurassic of Southern Germany).* In: Reitner J, Neuweiler F, Gunkel F (ed) Global and regional controls on biogenic sedimentation. I. Reef Evolution. Research Reports-Göttinger Arb. Geol. Paläont., Sb2:203-205
5. Choquette P.W., James N.P., 1990, *Limestones - The Burial Diagenetic Environment*, Geoscience Canada: 75-112.
6. Clari P., Martire L., 1996, *Interplay of cementation, mechanical compaction, and chemical compaction in nodular limestones of the Rosso Ammonitico Veronese (Middle-Upper Jurassic, northeastern Italy)*, Journal of Sedimentary Reasearch, 66: 447-458.
7. Czerniakowski L.A., Lohmann K.C., Wilson J.L., 1984, *Closed-system marine burial diagenesis: isotopic data from the Austin Chalk and its components*, Sedimentology 31:863-877.
8. Doglioni C., Goldhammer R.K., 1988, *Compaction-induced subsidence in the margin of a carbonate platform*, Basin Research, 1: 237-246.
9. Dżułyński S., 1952, The origin of the limestones in the Cracow area. Rocz Pol Tow Geol 21:125- 180 (in Polish with English summary).
10. Flügel E., 2004, *Microfacies of carbonate rocks, Analysis, Interpretation and Application*, Springer, New York, 1-976.

11. Garrison R.E., 1981, *Diagenesis of oceanic carbonate sediments: a review of the DSDP perspective.* In: Warme RE, Douglas RG, Winterer EL (ed) The Deep Sea Drilling Project: a Decade of Progress, Spec. Publ. Soc. Econ. Paleont. Miner. 32:181-207.
12. Goldhammer R.K., 1997, *Compaction and decompaction algorithms for sedimentary carbonates*, Journal of Sedimentary Reasearch, 67: 26-35.
13. Hunt D., Allsop T., Swarbrick R.E., 1996, *Compaction as a primary control on the architecture and development of depositional sequences: conceptual framework, applications and implications*, High Resolution Sequence Stratigraphy: Innovations and Applications, 104: 321-345.
14. Katsman R., Aharonow E., 2006, *A study of compaction bands originating from crack, notches, and compacted defects*, Journal of Structural Geology, 28: 508-518.
15. Kochman A., 2006, *Wybrane metody szacowania kompakcji w osadach węglanowych*, Technika Poszukiwań Geologicznych, Geotermia, Zrównoważony Rozwój, 238, 2: 35-45.
16. Kochman A., 2010, *Influence of compaction on the facial architecture of the Upper Jurassic basin of the southern part of the Krakow-Czestochowa Upland*, doctoral dissertation, AGH University of Science and Technology, Kraków, 117 p.
17. Krajewski M., Matyszkiewicz J., 2004, *Development and facial architecture of the Upper Jurassic complexes of buildups in the SW part of the Kraków Upland.* In: Partyka J (ed) Zróżnicowanie i przemiany środowiska przyrodniczo-kulturowego Wyżyny Krakowsko-Częstochowskiej, Tom I, Przyroda. Wyd. Ojcowski Park Narodowy, Ojców (in Polish with English summary).
18. Martire L., Clari P., 1994, *Evaluation of sedimentation rates in Jurassic-Cretaceous pelagic facies of the Trento Plateau: relevance of discontinuities and compaction*, Giornale di Geologia, 56, 2: 193-209.
19. Matyszkiewicz J., 1997, *Microfacies, sedimentation and some aspects of diagenesis of Upper Jurassic sediments from the elevated part of the Northern peri-Tethyan Shelf, a comparative study on the Lochen area (Schwäbische Alb) and the Cracow area (Cracow-Wielun Upland, Poland)*, Berlin Geowiss Abh, E 21: 1-111.
20. Matyszkiewicz J., 1999, *Sea-bottom relief versus differential compaction in ancient platform carbonates: a critical reassessment of an example from Upper Jurassic of the Cracow-Wieluń Upland*, Ann Soc Geol Polon 69:63-79.
21. Matyszkiewicz J., Krajewski M., Gołębiowska B., Jędrys J., Kochman A., Rzepa G., 2007, *Rozwój i ewolucja oksfordzkich budowli węglanowych w Zalasie*, Tomy Jurajskie 4:77-86 (in Polish)
22. Moore C.H., 2001, *Carbonate Reservoirs, Porosity Evolution and Diagenesis in Sequence Stratigraphic Framework*, Elsevier Science Publ., Amsterdam, 1-460.
23. Ricken W., 1986., *Diagenetic Bedding, A Model for Marl-limestone Alternations*, Springer, Berlin, 1-210.
24. Ricken W., 1987., *The carbonate compaction law: a new tool*, Sedimentology, 34: 571-584.
25. Rusciadelli G, Di Simone S., 2007, *Differential compaction as a control on depositional architectures across the Maiella carbonate platform margin (central Apennines, Italy)*, Sed Geol 196:133-155.
26. Saller A.H., 1996, *Differential compaction and basinward tilting of the prograding Capitan reef complex, Permian, west Texas and southeast New Mexico, USA*, Sed Geol 101:21-30.
27. Schlanger S.O., Douglas R.G., 1974, *The pelagic ooze-chalk-limestone transition and its implications for marine stratigraphy*, In: Hsü KJ, Jenkyns HC (ed) Pelagic Sediments, Spec. Publ. Int. Ass. Sediment. 1:117-148.
28. Shinn E.A., Robbin D.M., 1983, *Mechanical and chemical compaction in fine-grained shallow-water limestones*, Journal of Sedimentary Petrology, 53: 595-618.
29. Tucker M.E., Wright V.P., 2004, *Carbonate sedimentology*, Blackwell Science, Oxford, 1-491.
30. Westphal H., 1997, *Carbonate Platform Slopes - A Record of Changing Conditions, The Pliocene of the Bahamas*, Springer. Berlin-Heidelberg-New York, 1-197.